



This is the **submitted version** of the article:

Blázquez Palli, Natàlia; Shouakar-Stash, Ofan; Palau, Jordi; [et al.]. «Use of dual element isotope analysis and microcosm studies to determine the origin and potential anaerobic biodegradation of dichloromethane in two multi-contaminated aquifers». *Science of the total environment*, Vol. 696 (Dec. 2019), art. 134066. DOI 10.1016/j.scitotenv.2019.134066

This version is available at <https://ddd.uab.cat/record/212956>

under the terms of the  license

1 Use of dual element isotope analysis and microcosm
2 studies to determine the origin and potential anaerobic
3 biodegradation of dichloromethane in two multi-
4 contaminated aquifers

5 Natàlia Blázquez-Pallí^{a,b}, Orfan Shouakar-Stash^{c,d,e}, Jordi Palau^{f,g}, Alba Trueba-
6 Santiso^a, Joan Varias^b, Marçal Bosch^b, Albert Soler^f, Teresa Vicent^a, Ernest Marco-
7 Urrea^{a,*} and Mònica Rosell^f

8 ^a Departament d'Enginyeria Química, Biològica i Ambiental, Universitat Autònoma de
9 Barcelona (UAB), c/ de les Sitges s/n, 08193 Cerdanyola del Vallès, Spain.

10 ^b Litoclean, S.L., c/ Numància 36, 08029 Barcelona, Spain.

11 ^c Department of Earth and Environmental Sciences, University of Waterloo, Waterloo,
12 Ontario N2L 3G1, Canada

13 ^d Isotope Tracer Technologies Inc., Waterloo, Ontario N2 V 1Z5, Canada

14 ^e School of Engineering, University of Guelph, Guelph, Ontario, N1G 2W2, Canada

15 ^f Grup MAiMA, SGR Mineralogia Aplicada, Geoquímica i Geomicrobiologia,
16 Departament de Mineralogia, Petrologia i Geologia Aplicada, Facultat de Ciències de la
17 Terra, Institut de Recerca de l'Aigua (IdRA), Universitat de Barcelona (UB), c/ Martí
18 Franquès s/n, 08028 Barcelona, Spain.

19 ^g Institute of Environmental Assessment and Water Research (IDAEA), CSIC, Jordi
20 Girona 18-26, 08034 Barcelona, Spain

21

22 *Corresponding author:

23 Departament d'Enginyeria Química, Biològica i Ambiental, Universitat Autònoma de
24 Barcelona (UAB), c/ de les Sitges s/n, 08193 Cerdanyola del Vallès, Spain. E-mail:
25 ernest.marco@uab.cat, Phone: +34 935812694.

26 **Abstract**

27 Many aquifers around the world are impacted by toxic chlorinated methanes derived from
28 industrial processes due to accidental spills. Frequently, these contaminants co-occur with
29 chlorinated ethenes and/or chlorinated benzenes in groundwater, forming complex
30 mixtures that become very difficult to remediate. In this study, a multi-method approach
31 was used to provide lines of evidence of natural attenuation processes and potential
32 setbacks in the implementation of bioremediation strategies in multi-contaminated
33 aquifers. First, this study determined i) the carbon and chlorine isotopic compositions
34 ($\delta^{13}\text{C}$, $\delta^{37}\text{Cl}$) of several commercial pure phase chlorinated compounds, and ii) the
35 chlorine isotopic fractionation ($\epsilon_{\text{Cl}} = -5.2 \pm 0.6\text{‰}$) and the dual C–Cl isotope correlation
36 ($\Lambda^{\text{C/Cl}} = 5.9 \pm 0.3$) during dichloromethane (DCM) degradation by a *Dehalobacterium*-
37 containing culture. Such data provide valuable information for practitioners to support
38 the interpretation of stable isotope analyses derived from polluted sites. Second, the
39 bioremediation potential of two industrial sites contaminated with a mixture of organic
40 pollutants (mainly DCM, chloroform (CF), trichloroethene (TCE), and mono-
41 chlorobenzene (MCB)) was evaluated. Hydrochemistry, dual (C–Cl) isotope analyses,
42 laboratory microcosms, and microbiological data were used to investigate the origin, fate
43 and biodegradation potential of chlorinated methanes. At Site 1, $\delta^{13}\text{C}$ and $\delta^{37}\text{Cl}$
44 compositions from field samples were consistent with laboratory microcosms, which
45 showed complete degradation of CF, DCM and TCE, while MCB remained.
46 Identification of *Dehalobacter* sp. in CF-enriched microcosms further supported the

47 biodegradation capability of the aquifer to remediate chlorinated methanes. At Site 2,
48 hydrochemistry and $\delta^{13}\text{C}$ and $\delta^{37}\text{Cl}$ compositions from field samples suggested little
49 DCM, CF and TCE transformation; however, laboratory microcosms evidenced that their
50 degradation was severely inhibited, probably by co-contamination. A dual C-Cl isotopic
51 assessment using results from this study and reference values from the literature allowed
52 to determine the extent of degradation and elucidated the origin of chlorinated methanes.

53

54

55

56

57 1. Introduction

58 Dichloromethane (DCM) is a probable human carcinogen (IARC, 2016), included in the
59 list of priority pollutants of both the U.S. Agency for Toxic Substances and Disease
60 Registry (2016) and the European Commission (2012). DCM can be naturally released
61 by oceanic sources, wetlands, volcanoes and macroalgae (Gribble, 2010), but its detection
62 in groundwater is often a result of its extensive use, accidental spills and improper storage
63 in chemical, pharmaceutical, and petroleum industrial facilities, among others (Marshall
64 and Pottenger, 2016).

65 Numerous bacteria capable of using DCM as a growth substrate under aerobic
66 conditions have been identified, including various strains of *Hyphomicrobium* (Heraty et
67 al., 1999; Hermon et al., 2018; Nikolausz et al., 2006) and *Methylobacterium*
68 (Torgonskaya et al., 2019). The aerobic pathway for DCM biodegradation begins with a
69 glutathione S-transferase producing formaldehyde, which is partially oxidized to CO₂ and
70 chloride (Muller et al., 2011). To date, anaerobic biodegradation of DCM has been solely
71 reported for bacteria affiliated with the *Peptococcaceae* family: *Dehalobacterium*,
72 *Dehalobacter*, and *Candidatus Dichloromethanomonas elyunquensis* (*D. elyunquensis*).
73 *Dehalobacterium formicoaceticum* (*Dhb f.*) is the only pure culture described using DCM
74 as carbon and energy source under anoxic conditions, and produces formate and acetate
75 as end products (Mägli et al., 1998). Recently, mixed bacterial cultures containing
76 *Dehalobacter* sp. and/or *D. elyunquensis* have been reported to ferment DCM to mainly
77 acetate (Chen et al., 2017; Justicia-Leon et al., 2012; Kleindienst et al., 2017; Lee et al.,
78 2015, 2012).

79 Besides direct release into groundwater, DCM can also be produced by
80 dehalogenation of the higher chlorinated methanes (CMs), i.e. carbon tetrachloride (CT)
81 or chloroform (CF). The latter is listed as a probable carcinogen and a priority

82 contaminant as well (ATSDR, 2016; European Commission, 2012; IARC, 2018). Under
83 anoxic conditions, DCM might derive either from the hydrogenolysis of CF by the
84 organohalide-respiring bacteria *Dehalobacter* sp. and *Desulfitobacterium* sp. (Chan et al.,
85 2012; Ding et al., 2014; Tang and Edwards, 2013; Wong et al., 2016). Also, the anaerobic
86 degradation of CF by *Acetobacterium* sp. comprises both a reductive branch leading to
87 DCM and an oxidative pathway leading to CO₂ (Egli et al., 1990, 1988; Wanner et al.,
88 2018). DCM can be also produced co-metabolically by, for example, *Methanosarcina* sp.
89 or *Clostridium* sp. (Egli et al., 1988; Gälli and McCarty, 1989; Krone et al., 1989b, 1989a;
90 Mikesell and Boyd, 1990).

91 Chlorinated solvents are commonly found in complex mixtures in groundwater from
92 contaminated sites rather than as individual chemicals. In multi-contaminated aquifers,
93 microbial degradation can be affected and even inhibited by co-contaminants. This
94 information is relevant to foresee the efficiency of natural attenuation or enhanced
95 bioremediation strategies. For instance, the inhibitory effects of CF on key microbial
96 processes such as methanogenesis and microbial dechlorination reactions of chlorinated
97 ethenes (CEs) and ethanes are well known (Weathers and Parkin, 2000; Wei et al., 2016).
98 In addition, it has also been reported that CT and CF inhibit their mutual biodegradation
99 (da Lima and Sleep, 2010; Grostern et al., 2010; Justicia-Leon et al., 2014).

100 Compound-specific isotope analysis (CSIA) is a useful tool that allows
101 bioremediation practitioners to assess the effectiveness of remediation treatments. During
102 chemical or biological degradation of target contaminants, bonds containing the lighter
103 isotopes are preferentially broken, causing the remaining contaminant to be enriched in
104 the heavier isotopes compared to the original isotopic value (Aelion et al., 2009). This is
105 quantified through the abundance ratio of specific stable isotopes (e.g. ¹³C/¹²C, ³⁷Cl/³⁵Cl)
106 in contaminant molecules relative to an international standard (Aelion et al., 2009). This

107 technique may be used for source apportionment as well as the monitoring of
108 transformation processes in the field (Elsner, 2010). In addition, a quantitative estimation
109 of contaminant transformation extent in the field can be possible, provided that the isotope
110 fractionation (ϵ) for a given compound and degradation pathway are known and well
111 constrained (Aelion et al., 2009).

112 Dual element isotope analysis has some advantages over a single element isotope
113 approach. On the one hand, by improving the identification of the source (either related
114 to commercial solvents release or from parent compound degradation); on the other, by
115 allowing the elucidation of the fate of pollutants in the field. During biodegradation
116 processes, single element intrinsic isotope effects related to C–Cl bond cleavage can be
117 masked due to the occurrence of previous rate-limiting steps such as preceding enzymatic
118 reactions (Sherwood Lollar et al., 2010), bioavailability of electron donor and/or acceptor
119 (Aeppli et al., 2009; Kampara et al., 2008; Thullner et al., 2008), substrate uptake and
120 transport through the cell membrane (Cichocka et al., 2007; Renpenning et al., 2015),
121 among others. These processes are generally non- or slightly-isotope fractionating so that
122 both elements (e.g. C and Cl) are affected similarly. In this case, by taking the ratio of the
123 isotope shift for the two elements (e.g. $\Lambda = \Delta\delta^{13}\text{C} / \Delta\delta^{37}\text{Cl}$), their masking effect is
124 cancelled out and these slopes reflect better the ongoing degradation mechanisms (Elsner,
125 2010). While single element isotope fractionation could provide insight into the
126 underlying reaction mechanisms in laboratory biodegradation experiments, this is not
127 possible under field conditions. The reason is that contaminant concentration changes at
128 the field are also related to processes other than its transformation (such as sorption and
129 hydrodynamic dispersion), preventing accurate calculation of ϵ values. Thus, Λ values
130 determined from laboratory studied reactions can be compared with those obtained from
131 groundwater samples to investigate degradation processes at the field scale (Badin et al.,

132 2014; Hermon et al., 2018; Hunkeler et al., 2009; Palau et al., 2017; Rodríguez-Fernández
133 et al., 2018b).

134 Several laboratory studies have applied dual C–Cl isotope analysis to describe biotic
135 and abiotic transformation mechanisms for DCM (Chen et al., 2018; Heraty et al., 1999;
136 Torgonskaya et al., 2019) and CF (Heckel et al., 2019, 2017a; Rodríguez-Fernández et
137 al., 2018a; Torrentó et al., 2017) but, to the best of the author’s knowledge, the application
138 of a dual isotope approach in DCM-contaminated sites has not been reported yet.

139 The purpose of the work presented herein is two-fold. First, it aims to determine i) the
140 $\Lambda^{C/Cl}$ value for the anaerobic degradation of DCM by a *Dehalobacterium*-containing
141 culture, and ii) the carbon and chlorine isotopic compositions ($\delta^{13}C$, $\delta^{37}Cl$) of several
142 commercial pure phase DCM and CF. These new isotope data enrich the database to
143 which dual C–Cl isotopes slopes measured in the field can be compared to elucidate
144 degradation mechanisms. Second, a multi-method approach was used at two industrial
145 sites impacted by DCM, CF, trichloroethene (TCE) and mono-chlorobenzene (MCB) to
146 investigate their origin, fate and intrinsic biodegradation potential. To this end,
147 hydrochemical conditions in groundwater, concentrations of target contaminants and their
148 stable isotope ratios ($\delta^{13}C$, $\delta^{37}Cl$) in field samples were analysed. Afterwards, a dual C–
149 Cl isotopic assessment using the results from this study and reference values from the
150 literature was performed to reveal the origin and fate of DCM. Lastly, field-derived
151 microcosms testing for biostimulation as well as bioaugmentation, and 16S rRNA high-
152 throughput sequencing were performed to assess the intrinsic biodegradation potential of
153 target contaminants at the sites.

154

155 **2. Materials and methods**

156 *2.1. Materials*

157 Pure phase chlorinated compounds isotopically characterised and/or used for the
158 experiments were purchased at the highest purity available from the following suppliers:
159 CF (Sigma Aldrich, Alfa, Merck), DCM (Sigma Aldrich, Fisher, SDS, Merck), MCB
160 (Sigma Aldrich) and TCE (Panreac). CF (Sigma Aldrich) was used for the enrichment of
161 field-derived cultures. Industrial grade sodium L-lactate (97% purity, at 60% w/w) was
162 from Purac (Corbion). All other chemicals and reagents used were of the highest purity
163 available.

164 Samples of the time-course degradation of DCM in a culture containing
165 *Dehalobacterium (Dhb)* were obtained from a previous study reported elsewhere
166 (Trueba-Santiso et al., 2017).

167 Two different commercial bacterial consortia were used for the microcosm
168 bioaugmentation tests. Detailed information about the products cannot be disclosed due
169 to commercial confidentiality reasons. Commercial inoculum "S" was reported to
170 degrade CF to DCM, and fully dechlorinated CEs to ethene (ETH). Commercial inoculum
171 "M" was reported to degrade CF to methane via DCM and chloromethane.

172 *2.2. Hydrogeochemistry of the studied sites*

173 The sites are located in the Catalan Coastal Ranges, which are characterized by an
174 echelon fault system, subparallel to the coast, that affected the Hercynian basement and
175 the Mesozoic overlying sediments. The Neogene extension created a "horst and graben"
176 system filled by Miocene and Quaternary sediments. Both sites are located in the Neogene
177 basin, one of them in the Miocene sediments and the other in the granitic basement.

178 **Site 1**

179 The studied site is located at an industrial area in the Barcelona province (Spain).
180 Geologically, it is constituted by clays and conglomerates of quaternary age overlying
181 unconformable upper Miocene siliciclastic sediments that dip 15–20° in the NW
182 direction. Petrologically, the Miocene sediments are represented by clay and sands
183 composed of abundant quartz grains, mica and kaolinized feldspars and, locally, by some
184 conglomerates. Hydrogeologically, Miocene aquifer has an average transmissivity of 5–
185 180 m²/d, less than the alluvial aquifer. A geological cross section of the studied area can
186 be found in Section A of the Supporting Information (SI).

187 A previous characterization of the site detected high loads of contaminants and dense
188 nonaqueous phase liquid (DNAPL) in groundwater, which was originated after improper
189 storage of the substances (Figure 1A, SI section A). The main organic halogenated
190 compounds included DCM, CF, TCE, and MCB, but *cis*-1,2-dichloroethene (*cis*-DCE),
191 vinyl chloride (VC), tetrachloroethene (PCE), acetone, BTEX, and tetrahydrofuran were
192 also detected. The contamination plume was considered finite and contained. After the
193 initial site characterization, a pump and treat (P&T) remediation system (groundwater
194 extraction) was implemented. Under this ongoing treatment, groundwater flowed radially
195 towards the extraction points and a total of seven conventional fully screened monitoring
196 wells were sampled (Figure 1A, SI section B).

197 **Site 2**

198 This site is also located at an industrial zone in the Barcelona province (Spain), but
199 more than 30 km apart from Site 1. Geologically, it is constituted by Quaternary alluvial
200 sediments represented by sands and gravels that overlie unconformably the basement of
201 the Neogen basin made by later-Hercynian intrusive granites. Hydrogeologically,
202 groundwater flows mainly from the alluvial gravels to the river freshwater and, to a lesser
203 extent, through the more fractured and weathered granite. A conceptual site model of the

204 studied area can be found in SI section C.

205 Like in Site 1, it was previously confirmed that the aquifer in Site 2, originally
206 contaminated because of improper management, contained DNAPL (Figure 2A, SI
207 section C). The most abundant contaminants in groundwater included DCM, CF, TCE,
208 and MCB, but acetone, toluene, PCE, CT, VC, tetrahydrofuran and benzene were also
209 detected in groundwater. After the initial site characterization, dual-phase extraction
210 (DPE) and P&T remediation systems were implemented and ongoing during this study.
211 For the hydrochemical characterization, nine conventional fully screened monitoring
212 wells were sampled (Figure 2A, SI section D). At that time, the groundwater flow
213 direction was E–W, and radially towards the extraction points due to DPE and P&T, and
214 the contamination source was reported to be still active (SI section D).

215 2.3. Collection of groundwater samples

216 Hydrochemical parameters (Eh, pH, T and electric conductivity) were measured *in-*
217 *situ* and groundwater samples from selected monitoring wells (see SI sections B and D)
218 were collected as described elsewhere (Blázquez-Pallí et al., 2019). It has to be taken into
219 account that these values are an average of the screen length. Samples for chemical and
220 isotopic analysis were collected in different sampling containers on July 11th and 12th,
221 2017, from Site 1 and Site 2. Groundwater was collected with a peristaltic pump or bailer,
222 depending on the water table depth. Samples for C–Cl CSIA were preserved with HNO₃
223 (pH~2) (Badin et al., 2016) to prevent biodegradation processes. For the microcosm
224 experiments, groundwater with fine sediments from PZ-9, PZ-19 and PZ-36 from Site 2
225 (SI section D) and PI-2 from Site 1 (SI section B) was sampled on the 18th and 19th of
226 June 2018, respectively. All samples were collected in amber glass bottles sealed with
227 PTFE caps and stored in the dark at 4°C until used.

228 *2.4. Set up of laboratory microcosms*

229 The microcosms were prepared within the following two days after sampling. They
230 consisted of 65 mL of sampled groundwater in 100 mL glass serum sterile bottles sealed
231 with Teflon-coated butyl rubber septa as described elsewhere (Blázquez-Pallí et al.,
232 2019). To investigate whether a potential bioremediation treatment would be feasible at
233 the investigated sites, three different experiments were prepared in triplicate: (i) a control
234 containing only groundwater from the site, which tested for monitored natural attenuation
235 (MNA); (ii) groundwater with sodium lactate (~4 mM), which tested for biostimulation;
236 and (iii) groundwater inoculated with the commercial bacterial consortia described above
237 (10^6 – 10^7 cells/mL) plus sodium lactate (~4 mM), which tested for bioaugmentation. For
238 the samples from wells PZ-19 and PZ-36 (Site 2, SI section D), two different
239 bioaugmentation tests were established, i.e. one with each commercial inoculum, whereas
240 only one bioaugmentation test (using the commercial inoculum “S”) was performed with
241 samples from PZ-9 (Site 2, SI section D) and PI-2 (Site 1, SI section B).

242 To identify the bacteria responsible for CF degradation, the dilution-to-extinction
243 method (Löffler et al., 2005) was applied in 12-mL vials containing an anoxic defined
244 medium described elsewhere (Martín-González et al., 2015) and using CF as electron
245 acceptor. After four extinction series, the more diluted vial showing activity against CF
246 was used as inoculum for serum bottle microcosms, which were selected for 16S rRNA
247 analysis after consuming 1 mM CF. The serum bottle microcosms were prepared as
248 described elsewhere (Martín-González et al., 2015).

249 *2.5. DNA extraction and 16S rRNA gene amplicon sequencing*

250 Biomass was harvested from whole serum bottle microcosms in sterile falcon tubes
251 that were centrifuged for 40 min at $7000 \times g$ and 10 °C in an Avanti J-20 centrifuge. The

252 pellets were resuspended in sterile PBS buffer and, afterwards, DNA was extracted with
253 the Gentra Puregene Yeast/Bact kit (Qiagen) following the instructions of the
254 manufacturer. Extraction and analysis of the DNA of each microcosm was performed
255 separately. The regions V3–V4 of the 16S rRNA genes were amplified with primers S-
256 D-Bact-0341-b-S-17 and S-D-Bact-0785-a-A-21 (Klindworth et al., 2013) with the
257 Illumina MiSeq platform at *Serveis de Genòmica i Bioinformàtica* from *Universitat*
258 *Autònoma de Barcelona*.

259 2.6. Analytical methods

260 The hydrogeochemical parameters of groundwater (temperature, pH, redox potential
261 (Eh) and electric conductivity) were determined *in-situ* using a multiparameter probe
262 3430 WTW (Weilheim) as described elsewhere (Blázquez-Pallí et al., 2019).

263 Chlorinated compounds were quantified by analysing 500 μL of headspace samples
264 by gas chromatography (GC) coupled to a flame ionization detector (FID), as described
265 elsewhere (Martín-González et al., 2015). Lactate, acetate and other short-chain fatty
266 acids (VFAs) were monitored by HPLC from 1 mL filtered liquid samples (0.22 μm ,
267 Millex), as previously reported (Mortan et al., 2017).

268 Stable carbon isotope ratios ($\delta^{13}\text{C}$) of pure in-house standards were determined with a
269 Flash EA1112 (Carlo-Erba, Milano, Italy) elemental analyser (EA) coupled to a Delta C
270 isotope ratio mass spectrometer (IRMS) through a Conflo III interface (Thermo Finnigan,
271 Bremen, Germany), while the $\delta^{13}\text{C}$ values of target chlorinated compounds (DCM, CF,
272 CEs and MCB) in field samples were obtained by CSIA using an Agilent 6890 GC
273 coupled to a Delta Plus IRMS, as described in Blázquez-Pallí et al. (2019). All analyses
274 (standards and experimental samples) had a one standard deviation (1σ) lower than 0.5‰.

275 Stable chlorine isotope ratios ($\delta^{37}\text{Cl}$) were obtained by CSIA at Isotope Tracer

276 Technologies Inc., Waterloo (ON, Canada). A 6890 GC (Agilent, Santa Clara, CA, U.S.)
 277 coupled to a MAT 253 IRMS (Thermo Finnigan, Bremen, Germany) were used. This
 278 IRMS, equipped with nine collectors, is a continuous flow IRMS with a dual-inlet (DI)
 279 mode option. The DI bellows are used as the monitoring gas reservoir (either CF or DCM)
 280 and reference peaks were introduced at the beginning of each analysis run (Shouakar-
 281 Stash et al., 2006). For the analysis of chlorine isotope ratios of CF, the two main ion
 282 peaks (m/z 83 and 85) were used, which correspond to isotopologue pairs that differ by
 283 one heavy chlorine isotope ($[^{35}\text{Cl}_2^{12}\text{C}^1\text{H}]^+$ and $[^{37}\text{Cl}^{35}\text{Cl}^{12}\text{C}^1\text{H}]^+$, respectively) (Breider
 284 and Hunkeler, 2014). For DCM, the chlorine isotopic composition was determined from
 285 two ion peaks of the molecular group (m/z 84 and 86) corresponding to $[^{35}\text{Cl}_2^{12}\text{C}^1\text{H}_2]^+$
 286 and $[^{37}\text{Cl}^{35}\text{Cl}^{12}\text{C}^1\text{H}_2]^+$, respectively. Similarly to carbon isotopes analysis, the analytes
 287 were extracted by headspace solid-phase microextraction, as shown elsewhere (Palau et
 288 al., 2017). Samples and standards were diluted at similar concentrations and measured in
 289 duplicate. The $\delta^{37}\text{Cl}$ values of pure in-house standards were characterized relative to
 290 SMOC (Standard Mean Ocean Chloride) by offline IRMS analysis after conversion of
 291 DCM to methyl chloride according to Holt et al. (1997). These standards were later used
 292 to correct all measurements from samples. Precision (1σ) of the analysis was $\leq 0.2\text{‰}$ for
 293 $\delta^{37}\text{Cl}$.

294 The isotopic compositions of carbon and chlorine are reported in delta notation ($\delta^h\text{E}$,
 295 in ‰), relative to the international standards VPDB (Vienna Pee Dee Belemnite) and
 296 SMOC (Coplen, 1996; Kaufmann et al., 1984), respectively (Eq. 1),

$$\delta^h E = \left(\frac{R_{\text{sample}}}{R_{\text{std}}} - 1 \right) \quad (1)$$

298 where R_{sample} and R_{std} are the isotope ratios (i.e. $^{13}\text{C}/^{12}\text{C}$, $^{37}\text{Cl}/^{35}\text{Cl}$) of the sample and the
 299 standard of an element E, respectively (Elsner, 2010).

300 2.7. Calculations for interpretation of isotopic data

301 A simplified version of the Rayleigh equation in the logarithmic form (Eq. 2) correlates
302 changes in the isotopic composition of an element in a compound (R_t/R_0) with changes in
303 its concentration for a given reaction ($f = C_t/C_0$), which allows to determine the
304 corresponding isotopic fractionation (ε) (Coplen, 2011; Elsner, 2010).

305
$$\ln\left(\frac{R_t}{R_0}\right) = \varepsilon \cdot \ln(f) \quad (2)$$

306 R_t/R_0 can be expressed as $(\delta^h E_t + 1) / (\delta^h E_0 + 1)$ according to $\delta^h E$ definition. For the
307 experiment of DCM degradation by the stable enrichment culture containing *Dhb*, the ε_{Cl}
308 was obtained from the slope of the linear regression according to Eq. 2. The uncertainty
309 corresponds to the 95% confidence interval (CI).

310 For a target contaminant, the extent of degradation (D%) in the field was evaluated
311 with Eq. 3, which is derived from the Rayleigh equation (Eq. 2),

312
$$D\% = \left[1 - \left(\frac{\delta^h E_t + 1000}{\delta^h E_0 + 1000} \right)^{\frac{1000}{\varepsilon E}} \right] \cdot 100 \quad (3)$$

313 where εE refers to the isotopic fractionation, $\delta^h E_t$ are the isotope data from groundwater
314 samples and $\delta^h E_0$ is the most depleted value found at the field site, assumed to be the most
315 similar to the original source. To this regard, differences in isotope values in the field for
316 both carbon and chlorine ($\Delta\delta^{13}C$, $\Delta\delta^{37}Cl$) must be $>2\%$ for degradation to be considered
317 significant (Hunkeler et al., 2008). Laboratory derived ε values can either be site-specific
318 (i.e., from microcosm experiments prepared with soil and/or groundwater from the
319 contaminated site) or obtained from the literature (Table 1).

320 Finally, the $\Lambda^{C/Cl}$ value for the DCM biodegradation experiment was obtained from
321 the slope of the linear regression in the dual C–Cl isotope plot (Elsner, 2010) and the

322 uncertainty is the 95% CI.

323 *2.8. Dual C–Cl isotopic assessment based on selected $\Lambda^{C/Cl}$*

324 To understand the origin and fate of DCM and CF at each site, a dual C–Cl isotopic
325 assessment (Badin et al., 2016; Hunkeler et al., 2008) was performed based on the
326 measured $\delta^{13}C$ and $\delta^{37}Cl$ data of field and commercial compounds, the definition of D%
327 (Eq. 3), and ϵC , ϵCl and $\Lambda^{C/Cl}$ from the available literature (Tables 1 and 2). The procedure
328 followed for the dual C–Cl isotopic assessment is detailed in SI section E.

329

330 **3. Results and discussion**

331 *3.1. $\delta^{13}C$ and $\delta^{37}Cl$ of pure in-house commercial standards*

332 Several pure in-house commercial standards were analysed to determine their $\delta^{13}C$ and
333 $\delta^{37}Cl$ compositions (see details in Table 2). $\delta^{13}C_{DCM}$ for the standards that were measured
334 in this study ranged from -35.4 ± 0.2 to $-41.71 \pm 0.08\text{‰}$, while $\delta^{37}Cl_{DCM}$ ranged from $+2.1$
335 ± 0.3 to $-2.7 \pm 0.1\text{‰}$. $\delta^{13}C_{CF}$ ranged from -47.96 ± 0.06 to $-52.7 \pm 0.1\text{‰}$, while $\delta^{37}Cl_{CF}$
336 ranged from -2.6 ± 0.1 to $-5.9 \pm 0.2\text{‰}$. A significant variation was observed among the
337 different DCM and CF commercial standards analysed in this study, but also when
338 compared to some of the values available in the literature. For instance, the $\delta^{37}Cl_{DCM}$
339 value obtained for the Fisher standard ($-2.7 \pm 0.1\text{‰}$) is more depleted in ^{37}Cl than the
340 values available to date (Table 2), emphasizing the relevance of reference isotopic
341 composition of the pure products provided in this study for future data interpretation.
342 Lastly, $\delta^{13}C$ for TCE and MCB was also analysed here and resulted in $-25.40 \pm 0.03\text{‰}$
343 and $-27.09 \pm 0.07\text{‰}$, respectively.

344 *3.2. Chlorine isotope fractionation and $\Lambda^{C/Cl}$ during anaerobic DCM degradation by a* 345 *Dhb-containing culture*

346 Samples of a *Dhb*-containing culture that were previously killed to analyse the
347 decrease of concentration and the carbon isotope fractionation of DCM (Trueba-Santiso
348 et al., 2017) were used in this study. The $\delta^{37}\text{Cl}$ during DCM degradation increased from
349 -5.7 ± 0.2 to $+7.2 \pm 0.2\text{‰}$ after 97% transformation, but neither changes in concentration
350 nor in $\delta^{37}\text{Cl}$ (average $-5.7 \pm 0.2\text{‰}$) were observed in the abiotic controls. However, this
351 last point (97%) was excluded because it appeared to be deviated from the linear
352 regression ($R^2=0.95$, Eq. 2), whereas the best-fitting was obtained for $\delta^{37}\text{Cl}$ values up to
353 84% degradation ($R^2=0.98$) leading to a ϵCl of $-5.2 \pm 0.6\text{‰}$ (Figure 3A). This
354 phenomenon was observed previously by Mundle et al. (2013), who reported higher
355 uncertainty in ϵ values calculated at later stages of the reaction and suggested examining
356 the linearity of the fits over shorter reaction progress intervals. To date, there is still no
357 ϵCl value available for *Dehalobacter*, but the ϵCl value of $-5.2 \pm 0.6\text{‰}$ obtained in this
358 study for *Dhb* is not significantly different from those reported for *D. elyunquensis* (-5.2
359 $\pm 0.1\text{‰}$), *Dhb f.* ($-5.3 \pm 0.1\text{‰}$), and purified dehalogenases of *M. extorquens* DM4 and
360 *Methylophilus leisingeri* DM11 (-5.7 and -5.6‰ , respectively) (Chen et al., 2018;
361 Torgonskaya et al., 2019) according to the student's *t*-test (8 degrees of freedom, $p=0.05$).
362 In contrast, it is significantly different than those reported for *Hyphomicrobium* sp. strain
363 MC8b (-3.8‰) and *Methylobacterium extorquens* DM4 (-7.0‰) (Heraty et al., 1999;
364 Torgonskaya et al., 2019) (Table 1).

365 The ϵC recalculated up to 84% degradation for *Dhb* ($-31 \pm 3\text{‰}$, $R^2=0.986$) does not
366 vary much from the previously published value ($-27 \pm 2\text{‰}$, $R^2=0.985$) (Trueba-Santiso et
367 al., 2017), and still differ from the reported DCM-fermentative bacteria *Dehalobacter* ($-$
368 $16 \pm 2\text{‰}$) (Lee et al., 2015). However, recent studies on *Hyphomicrobium* sp. strains
369 (Hermon et al., 2018) and *Methylobacterium extorquens* DM4 (Torgonskaya et al., 2019)
370 has widened the ϵC range attributed to methylotrophic bacteria (-22 to -66.6‰), not

371 allowing to distinguish hydrolytic transformation of DCM via glutathione-dependent
372 dehalogenases and fermentation pathway just by carbon isotopes.

373 A very good linear correlation ($R^2=0.995$) was also obtained for $\delta^{13}\text{C}$ against $\delta^{37}\text{Cl}$
374 values up to 84% degradation in a dual C–Cl isotope plot ($\Lambda^{\text{C/Cl}}$ of 5.9 ± 0.3 , Figure 3B).
375 This $\Lambda^{\text{C/Cl}}$ value by the *Dhb*-containing culture is significantly different from those
376 reported for *D. elyunquensis* ($\Lambda^{\text{C/Cl}} = 3.40 \pm 0.03$) and for *Dhb f.* ($\Lambda^{\text{C/Cl}} = 7.89 \pm 0.12$)
377 (Chen et al., 2018) (Figure 3B) according to the student's *t* test (8 degrees of freedom,
378 $p=0.05$). The difference between *Dhb* and *D. elyunquensis* is in accordance with recent
379 proteogenomic findings suggesting that both genera have distinct DCM degradation
380 pathways (Kleindienst et al., 2019). However, the difference observed between *Dhb* and
381 *Dhb f.* may suggest that they either have mechanistic disparities during DCM degradation,
382 even though they both belong to the same genus. Higher $\Lambda^{\text{C/Cl}}$ values, ranging from 8.1
383 to 11.2, have been reported for the aerobic *Hyphomicrobium* sp. strain MC8b (Heraty et
384 al., 1999), *Methylobacterium extorquens* DM4, and DM4 and DM11 DCM dehalogenases
385 (Torgonskaya et al., 2019). To date, these values hint at the distinction between aerobic
386 (11.2 to 8.1) and anaerobic (7.89 to 3.40) pathways (Figure 3B). However, further
387 research on this topic would be needed to confirm such hypothesis. See Table 1 for a
388 detailed review of literature values.

389

390 3.3. Field sites investigation

391

392 3.3.1. Site 1

393 The studied aquifer exhibited mixed redox conditions (Eh ranged from +250 to -52)
394 mV), but most of the wells were in anoxic conditions (SI section F), which are conducive

395 to reductive dechlorination reactions. Temperature and pH were considered homogeneous
396 throughout the aquifer (21.1 ± 0.7 °C and 6.8 ± 0.3 , respectively) (SI section F). CF was
397 the organohalide detected at the highest concentration (454 mg/L), followed by MCB
398 (82.7 mg/L), TCE (47.2 mg/L), and DCM (1.47 mg/L) (Figure 1A and SI section G).

399 The C–Cl isotopic composition of CF could be determined in 5 out of 7 monitoring
400 wells (Figure 1A). Obtained $\delta^{13}\text{C}$ values for CF showed a relatively small but significant
401 variation ($\Delta\delta^{13}\text{C}_{\text{CF}}$) of 3.2‰ between wells PI-17 and CV-5, which exhibited the most
402 enriched and depleted $\delta^{13}\text{C}_{\text{CF}}$, respectively (SI section H). Since the difference in the
403 carbon isotope composition was $>2\%$, it could be related to CF transformation in
404 groundwater (Hunkeler et al., 2008). In contrast, the maximum $\Delta\delta^{37}\text{Cl}_{\text{CF}}$ observed at the
405 site between wells CV-5 and PI-24 was lower than 2‰. This agrees well with previous
406 studies showing ϵC values usually greater than ϵCl during CF biodegradation (Table 1).
407 The dual isotopic composition of CF in the analysed groundwater samples fell outside the
408 isotopic range of commercial CF, except for samples collected in well CV-5 (SI section
409 I). This result would further support a potential transformation of CF at the site.

410 For DCM, only one C–Cl isotopic composition could be determined (in well PI-26)
411 due to DCM concentration being too low for carbon CSIA, but $\delta^{37}\text{Cl}$ could be determined
412 in 4 out of 7 wells (Figure 1A). Obtained $\delta^{37}\text{Cl}$ for DCM showed a significant variation
413 in $^{37}\text{Cl}/^{35}\text{Cl}$ ratios of $\Delta\delta^{37}\text{Cl}_{\text{DCM}} = 2.3\%$ between wells CV-5 and PI-26 (SI section H,
414 Figure 1A), and these $\delta^{37}\text{Cl}$ were enriched compared to those of commercial DCM (Table
415 2). As mentioned earlier, no $\Delta\delta^{13}\text{C}_{\text{DCM}}$ can be provided for $\delta^{13}\text{C}$ since only one value
416 could be obtained, but this value was also enriched compared to most of the $\delta^{13}\text{C}$ reported
417 for commercial DCM (Table 2). Hence, this dual C–Cl isotopic composition for DCM in
418 the analysed groundwater of well PI-26 fell outside the isotopic range of commercial
419 DCM, suggesting a potential transformation of DCM at the site as well (SI section I).

420 When comparing these results to the literature, the low carbon enrichment observed could
421 indicate that the bacteria responsible for DCM degradation have a ϵ_C that is in the lower
422 range (e.g. *Dehalobacter* sp., which has the lowest reported ϵ_C as presented in Table 1).
423 An additional evidence pointing towards *in-situ* DCM biodegradation was the detection
424 of acetate in wells PI-26 and CV-3 (Figure 1A and SI section G), which is the main by-
425 product of DCM fermentation (Justicia-Leon et al., 2012; Lee et al., 2015; Mägli et al.,
426 1998; Trueba-Santiso et al., 2017).

427 Interestingly, $\delta^{13}C_{TCE}$ in the wells that also contained CF ranged between -32.5 and -
428 31.8‰ but was significantly enriched in ^{13}C in the unique well (PI-3) that lacked CF
429 ($\delta^{13}C_{TCE} = -28.2\%$, Figure 1A). This may be in agreement with several studies suggesting
430 that CF can inhibit significantly microbial reductive dechlorination of CEs, as reviewed
431 elsewhere (Wei et al., 2016). However, *cis*-DCE, VC and ETH were also detected in most
432 of the monitored wells (SI section G) indicating that, despite this potential inhibition
433 effect suggested by the isotopic analysis, full dechlorination of TCE occurred.

434 Lastly, no significant carbon isotope fractionation was observed for MCB ($\Delta\delta^{13}C_{MCB}$
435 $< 2\%$, SI section H), and obtained $\delta^{13}C$ values were within the available range of
436 commercial MCB solvents (Table 2), indicating that this compound was, most likely, not
437 being degraded.

438 To investigate the biodegradation potential of the site, three different microcosm
439 treatments were prepared with groundwater from well PI-2 (SI section J). The non-
440 amended microcosms used as natural attenuation controls fully degraded CF and DCM,
441 and transformed TCE to VC after 75 days. The microcosms amended with either only
442 lactate (biostimulation) or also inoculated with “S” (bioaugmentation) increased the
443 degradation rate of CF (to DCM), DCM, TCE and, more importantly, fully dechlorinated
444 the latter to stoichiometric amounts of ETH. Both CMs and CEs elimination occurred

445 simultaneously (SI section J). These results confirmed the feasibility of *in-situ* CF, DCM
446 and TCE biodegradation, and agreed with the information obtained from the isotopic field
447 data that was just discussed. In contrast, MCB always accumulated in the medium of the
448 microcosms and was not degraded (SI section J). Such evidence further supports the
449 evidence obtained from the isotopic field data, which pointed towards the recalcitrance
450 of the pollutant. Thus, it could be discarded that benzene, which was detected in the
451 preliminary characterization of this aquifer, was derived from MCB biodegradation.
452 Regarding the amended substrate, lactate was converted to acetate (major product) and
453 propionate in all the amended microcosms (SI section K).

454 The composition of the microbial community was assessed by 16S rRNA high-
455 throughput sequencing. The analysis was performed on groundwater samples collected
456 from well PI-2 that were enriched with CF for four consecutive dilution series. The
457 taxonomic assignments of 16S rRNA sequences revealed that the four predominant
458 genera were *Clostridium* (31%), *Sedimentibacter* (25%), *Dehalobacter* (10%) and
459 *Acetobacterium* (4%) (SI section L). The presence of *Dehalobacter*, a well-known CF
460 and DCM degrader (Justicia-Leon et al., 2012; Lee et al., 2015), further supports the
461 intrinsic biodegradation potential of the aquifer to remediate CMs. In addition, results
462 also suggested that *Clostridium* sp. and *Acetobacterium* sp. could be somehow involved
463 in the degradation of CF as well, as described elsewhere (Egli et al., 1990, 1988; Gälli
464 and McCarty, 1989; Wanner et al., 2018).

465 With these evidences and aiming to better understand the origin and fate of CF and
466 DCM at this site, a dual C–Cl isotopic assessment was performed based on the assumption
467 that CF in well CV-5 reflected the initial isotopic signature (CF₀) since it possessed the
468 most depleted $\delta^{13}\text{C}$ and $\delta^{37}\text{Cl}$ values (Figure 1A). The dual isotope fractionation pattern
469 observed for CF in CV-3, PI-17 and PI-26 was consistent with the degradation of leaked

470 commercial CF, since the data points fell within the estimated potential isotopic
471 composition for degraded CF (orange area, Figure 1B). Accordingly, the values for DCM
472 initially produced from CF degradation (DCM_{ini}) ranged between -50.9‰ and -73.9‰
473 for $\delta^{13}C$ and was of -2.2‰ for $\delta^{37}Cl$ (Figure 1B, SI section E). The isotopic composition
474 of DCM detected in well PI-26 (SI section H) was enriched in ^{37}Cl compared to that of
475 commercial DCM (Table 2), and in both ^{13}C and ^{37}Cl compared to that of DCM produced
476 by CF degradation (SI section E), suggesting that it could be subject to biodegradation
477 (Figure 1B). However, regarding the main source of detected DCM at the site, obtained
478 results point to a potential spill of DCM at the site being more likely than DCM produced
479 by CF degradation, but neither could be confirmed.

480 In the above scenario, and assuming *Dehalobacter* sp. was the responsible for CF
481 biotransformation, the extent of biodegradation (D%) for CF estimated in the wells CV-
482 3, PI-17 and PI-26 (where $\Delta\delta^{13}C$ was $> 2\%$, SI section H) ranged between 7–11%
483 considering the ϵC data reported for *Dehalobacter* strain CF ($\epsilon C = -28 \pm 2$). Data for
484 *Dehalobacter* strain CF was used for this calculation because its $\Lambda^{C/Cl}$ was more coherent
485 with the field results from Site 1 (i.e. the isotopic pattern of positive dual C–Cl slopes
486 observed for CF measurements), than the $\Lambda^{C/Cl}$ of *Dehalobacter* strain UNSWDHB
487 (Table 1). Nevertheless, further research needs to be done on this culture to better
488 understand the roles of *Dehalobacter*, *Clostridium* and *Acetobacterium* bacteria, and
489 elucidate the biodegradation mechanisms of both CF and DCM, which would allow an
490 improved assessment and quantification of D% at the field.

491 3.3.2. Site 2

492 At this site, Eh ranged from +254 to -118 mV, but groundwater in most of the wells
493 exhibited oxic conditions which limit the occurrence of reductive dechlorination reactions
494 (SI section F). Temperature and pH were considered homogeneous and averaged 24 ± 2

495 °C and 6.8 ± 0.3 , respectively (SI section F). CF was detected at the highest concentrations
496 (272 mg/L), followed by DCM (27 mg/L), TCE (1.7 mg/L) and MCB (0.88 mg/L) (Figure
497 2A and SI section G).

498 $\delta^{13}\text{C}$ and $\delta^{37}\text{Cl}$ of CF could be determined in 7 out of 9 wells because the concentration
499 of CF in PZ-5 and PZ-31 was below the limit of quantification (Figure 2A). The $\Delta\delta^{13}\text{C}_{\text{CF}}$
500 $> 2\text{‰}$ observed between PZ-9 and PZ-18 wells and the $\Delta\delta^{37}\text{Cl}_{\text{CF}} < 2\text{‰}$ observed between
501 PZ-10 and PZ-18 wells (SI section H) could be related to CF transformation in
502 groundwater (Hunkeler et al., 2008) considering the low ϵ_{Cl} reported for CF
503 transformation. However, most of the C–Cl isotope compositions of CF were within the
504 isotopic range for commercial CF (SI section I), which could also indicate that measured
505 $\delta^{13}\text{C}$ and $\delta^{37}\text{Cl}$ belonged to a leaked and not degraded CF.

506 On its side, detected DCM presented a higher variation for both C and Cl isotope ratios
507 ($\Delta\delta^{13}\text{C}_{\text{DCM}} = 6.1\text{‰}$ between wells PZ-19 and PZ-36, $\Delta\delta^{37}\text{Cl}_{\text{DCM}} = 2.2\text{‰}$ between wells
508 PZ-9 and PZ-18, Figure 2A, SI section H) indicative of potential *in-situ* transformations.
509 In this case, however, the isotopic composition in well PZ-36 did fall within the
510 commercial DCM, whereas well PZ-19 did not (Figure 2B and SI section I, see further
511 discussion below).

512 For TCE, $\Delta\delta^{13}\text{C}$ was of 5.8‰ (SI section H), which could be related to TCE
513 transformation in groundwater (Hunkeler et al., 2008), and measured $\delta^{13}\text{C}_{\text{TCE}}$ values were
514 more enriched in ^{13}C than the $\delta^{13}\text{C}$ compositions of commercial TCE (Table 2), in
515 agreement with potential TCE degradation. However, the reductive dechlorination
516 products of TCE (DCE, VC, and ETH) were detected occasionally and at very low
517 concentrations (SI section G).

518 Microcosm experiments were prepared with groundwater from wells PZ-9, PZ-19 and

519 PZ-36. Microcosms for well PZ-9 did not show significant degradation of neither CF nor
520 CEs, and no major differences were observed between the non-amended, biostimulated
521 and the bioaugmented treatments after 150 days (SI section M). However, traces of DCM
522 and VC, a slight decrease in PCE and TCE, and formation of *trans*-DCE were observed
523 throughout the course of the study (SI section M). For PZ-19, no significant elimination
524 of contaminants was observed, although TCE did exhibit a decrease in all microcosms
525 and traces of *cis*-DCE, *trans*-DCE and VC were detected in some of them (SI section N).
526 For PZ-36, the non-amended, biostimulated and bioaugmented (with “M”) microcosms
527 did neither degrade CF nor CEs significantly. In contrast, the bioaugmented (with “S”)
528 treatment exhibited a CF decrease with the transient production of DCM, and TCE was
529 completely transformed to VC and *trans*-DCE (SI section O). Amended lactate was
530 mainly transformed to acetate in PZ-9 and PZ-36 microcosms. In PZ-19, however, lactate
531 was not completely consumed but, in both bioaugmentation tests, its decrease was
532 followed by acetate and propionate production (SI section K). The inability of inoculated
533 bacteria to efficiently degrade contaminants in these microcosms suggested that there
534 were inhibition issues, possibly due to the presence of co-contaminants in groundwater
535 such as CT, which is a known inhibitor of the microbial activity and CF degradation in
536 particular (section 2.2) (da Lima and Sleep, 2010; Grostern et al., 2010; Justicia-Leon et
537 al., 2014; Wei et al., 2016). The results obtained with the microcosms suggested that,
538 under the studied conditions, degradation of contaminants was very slow and inefficient,
539 but possible to some extent, which agreed with the information obtained from the isotopic
540 field data that was discussed above.

541 At this site, the dual C–Cl isotopic assessment was performed based on a CF₀ signature
542 of $\delta^{13}\text{C} = -45.1\text{‰}$ (from PZ-9) and $\delta^{37}\text{Cl} = -3.5\text{‰}$ (from PZ-10), as they were the most
543 depleted values measured (Figure 2A). The dual isotope fractionation pattern observed

544 for CF was not consistent with degradation (orange area, Figure 2B), in agreement with
545 the microcosms. However, it should be noted that $\delta^{37}\text{Cl}_{\text{CF}}$ values were enriched respect
546 to CF_0 signature. This could be attributable to Cl isotope fractionation processes in the
547 unsaturated zone due to diffusion-controlled vaporization (Jeannotat and Hunkeler,
548 2012; Palau et al., 2016) or to the leakage of CF from different providers with distinct
549 isotopic signatures. Moreover, it has to be taken into account that this release of CF was
550 still active at the site and potential CF degradation could be masked by a more depleted
551 CF input. In the hypothetical case that CF was biologically degraded, the calculated
552 isotopic range for DCM_{ini} (formation of DCM from CF degradation) would range from -
553 52.1‰ to -75.1‰ for carbon, and -3.5‰ for chlorine (Figure 2B, SI section E). The
554 isotopic composition of DCM detected in groundwater (Figure 2B, SI section H) was very
555 enriched in both ^{37}Cl and ^{13}C compared to that of initial DCM produced by CF
556 degradation (grey area, Figure 2B). In detail, DCM detected in PZ-36 (with the highest
557 DCM concentration, Figure 2A) was within the range of commercial DCM (Figure 2B),
558 pointing to a potential release of DCM at the site. However, this DCM could be subject
559 to a little biodegradation as acetate, the main by-product of DCM fermentation, was
560 detected in the well PZ-36 and also in PZ-18 (SI section G). For the well PZ-19, the
561 $\delta^{13}\text{C}_{\text{DCM}}$ value is slightly depleted in ^{13}C while the $\delta^{37}\text{Cl}_{\text{DCM}}$ value is lightly enriched in
562 ^{37}Cl compared to those measured in PZ-36 (Figure 2B). This could be explained similar
563 to CF, in this case DCM could be an impurity in the CF raw source with isotopic signature
564 changing over time due to change in CF providers or manufacturing processes or by the
565 effect of vaporization and diffusion processes in the unsaturated zone (Jeannotat and
566 Hunkeler, 2012; Palau et al., 2016). As noted above, the release of CF (and probably
567 DCM) was still active at the site. Taking all these evidences into account, the extent of
568 biodegradation (D%) for CF was not estimated since the results would not be

569 representative of CF degradation.

570

571 **4. Conclusions**

572 The present study provides additional data on isotope C and Cl compositions for
573 different commercial CMs, widening the known range for these solvents and proving the
574 utility of these results for data interpretation. In addition, the C and Cl isotopic
575 fractionation values for the anaerobic degradation of DCM by a *Dhb*-containing culture
576 were also determined. These results enrich the available database that can be used by
577 practitioners to provide diagnostic information about CMs biodegradation in
578 contaminated aquifers. The value of $\Lambda^{C/Cl}$ obtained for the investigated *Dhb*-containing
579 culture was right in between of those described for *Dhb f.* and *D. elyunquensis*, which
580 would allow the distinction of these DCM degradation mechanisms through isotope
581 analyses.

582 The pumping regimes that were active at both studied sites probably impacted the
583 geographical distribution of the chlorinated compounds and their corresponding isotopic
584 signatures. For this reason, the focus of this work was not on the flow path of the plume
585 but on the correlation between the isotopic composition of the chlorinated solvents and
586 the biodegradation information obtained from microcosms experiments for each
587 monitoring well. For this, the use of an integrative approach that combines C–Cl CSIA,
588 laboratory microcosms, and 16S rRNA high-throughput sequencing demonstrated the
589 intrinsic biodegradation potential of Site 1 to fully transform CF, DCM, and CEs, but not
590 MCB. In contrast, results for Site 2 suggested that inhibition was preventing the efficient
591 elimination of CMs and CEs at tested conditions. Nevertheless, the dual C–Cl isotopic
592 assessment proved useful, as well, to elucidate the origin and fate of DCM and CF at both

593 sites. Considering these results, a biostimulation (e.g. enhanced reductive dechlorination
594 with lactate) could be applied at Site 1 to degrade both CMs and CEs. However, the
595 persistence of MCB at this site, and the inhibition of biodegradation observed at Site 2,
596 suggest that a treatment train (i.e. a combination or sequence of different remedial
597 strategies targeting different groups of contaminants) could possibly be the optimal
598 approach for the detoxification of these aquifers.

599 This study shows that such a multi-method approach allows for the collection of data
600 that can help making decisions in the field. In this case, it is a valuable tool to evaluate
601 the feasibility of biodegradation strategies to remediate chlorinated solvents in complex
602 multi-contaminated aquifers, as it can provide the lines of evidence required to
603 demonstrate whether bacteria can successfully detoxify groundwater, and identify any
604 potential setbacks. The microcosm tests can provide a positive indication that complete
605 dechlorination can be achieved by native microbial populations, and is useful to predict
606 the effect of bioremediation treatments (biostimulation or bioaugmentation) to detoxify
607 the aquifer. Changes in carbon and chlorine isotope composition among the residual
608 fraction of the chlorinated compounds in the monitoring wells can provide field evidence
609 for microbial degradation. Lastly, the positive molecular identification of key
610 organohalide-respiring bacteria (e.g. *Dehalobacter*) can provide additional evidence that
611 chlorinated solvents can be fully dechlorinated in the aquifer. Notwithstanding, there is a
612 need for additional laboratory studies that correlate the metabolism of microbial
613 transformations with stable isotope fractionation of multiple elements to support the
614 interpretation of CSIA data obtained from contaminated groundwaters, as well as the
615 potential inhibitory effect of co-contaminants over bacteria degrading organochlorides.

616

617 **5. Acknowledgements**

618 This research has been supported by the Spanish State Research Agency (CTM2016-
619 75587-C2-1-R and CGL2017-87216-C4-1-R projects), co-financed by the European
620 Union through the European Regional Development Fund (ERDF). This work was also
621 partly supported by *Generalitat de Catalunya* through the consolidate research groups
622 (2017SGR-14 and 2017SGR-1733) and the Industrial Doctorate grant of N. Blázquez-
623 Pallí (2015-DI-064). A. Trueba-Santiso acknowledges support from a MICINN
624 predoctoral research grant (BES-2014-070817). M. Rosell acknowledges a *Ramón y*
625 *Cajal* contract (RYC-2012-11920) from MICINN. The *Departament d'Enginyeria*
626 *Química, Biològica i Ambiental* of *Universitat Autònoma de Barcelona* is a member of
627 the *Xarxa de Referència en Biotecnologia de la Generalitat de Catalunya*. The authors
628 thank Jessica M. Soder-Walz for her collaboration in the laboratory work.

629 **References**

- 630 Aelion, C.M., Höhener, P., Hunkeler, D., Aravena, R., 2009. Environmental Isotopes in
631 Bioremediation and Biodegradation. CRC Press, Boca Raton.
632 <https://doi.org/10.1159/000076616>
- 633 Aeppli, C., Berg, M., Cirpka, O.A., Holliger, C., Schwarzenbach, R.P., Hofstetter, T.B.,
634 2009. Influence of mass-transfer limitations on carbon isotope fractionation during
635 microbial dechlorination of trichloroethene. *Environ. Sci. Technol.* 43, 8813–8820.
636 <https://doi.org/10.1021/es901481b>
- 637 ATSDR, 2016. Substance priority list [WWW Document]. *Subst. Prior. List*. URL
638 <https://www.atsdr.cdc.gov/SPL/index.html> (accessed 10.31.17).
- 639 Badin, A., Broholm, M.M., Jacobsen, C.S., Palau, J., Dennis, P., Hunkeler, D., 2016.
640 Identification of abiotic and biotic reductive dechlorination in a chlorinated ethene
641 plume after thermal source remediation by means of isotopic and molecular biology
642 tools. *J. Contam. Hydrol.* 192, 1–19. <https://doi.org/10.1016/j.jconhyd.2016.05.003>
- 643 Badin, A., Buttet, G., Maillard, J., Holliger, C., Hunkeler, D., 2014. Multiple dual C–Cl
644 isotope patterns associated with reductive dechlorination of tetrachloroethene.
645 *Environ. Sci. Technol.* 48, 9179–9186. <https://doi.org/10.1021/es500822d>
- 646 Blázquez-Pallí, N., Rosell, M., Varias, J., Bosch, M., Soler, A., Vicent, T., Marco-Urrea,
647 E., 2019. Multi-method assessment of the intrinsic biodegradation potential of an
648 aquifer contaminated with chlorinated ethenes at an industrial area in Barcelona
649 (Spain). *Environ. Pollut.* 244, 165–173.
650 <https://doi.org/10.1016/j.envpol.2018.10.013>
- 651 Breider, F., 2013. Investigating the origin of chloroform in soils and groundwater using

652 carbon and chlorine stable isotopes analysis. Université de Neuchâtel (Switzerland).

653 Breider, F., Hunkeler, D., 2014. Investigating chloroperoxidase-catalyzed formation of
654 chloroform from humic substances using stable chlorine isotope analysis. *Environ.*
655 *Sci. Technol.* 48, 1592–1600. <https://doi.org/10.1021/es403879e>

656 Chan, C.C.H., Mundle, S.O.C., Eckert, T., Liang, X., Tang, S., Lacrampe-Couloume, G.,
657 Edwards, E., Sherwood Lollar, B., 2012. Large carbon isotope fractionation during
658 biodegradation of chloroform by *Dehalobacter* cultures. *Environ. Sci. Technol.* 46,
659 10154–10160. <https://doi.org/10.1021/es3010317>

660 Chen, G., Kleindienst, S., Griffiths, D.R., Mack, E.E., Seger, E.S., Löffler, F.E., 2017.
661 Mutualistic interaction between dichloromethane- and chloromethane-degrading
662 bacteria in an anaerobic mixed culture. *Environ. Microbiol.* 19, 4784–4796.
663 <https://doi.org/10.1111/1462-2920.13945>

664 Chen, G., Shouakar-Stash, O., Phillips, E., Justicia-Leon, S.D., Gilevska, T., Sherwood
665 Lollar, B., Mack, E.E., Seger, E.S., Löffler, F.E., 2018. Dual carbon-chlorine isotope
666 analysis indicates distinct anaerobic dichloromethane degradation pathways in two
667 members of the *Peptococcaceae*. *Environ. Sci. Technol.* 52, 8607–8616.
668 <https://doi.org/10.1021/acs.est.8b01583>

669 Cichocka, D., Siegert, M., Imfeld, G.G., Andert, J., Beck, K., Diekert, G., Richnow, H.H.,
670 Nijenhuis, I., 2007. Factors controlling the carbon isotope fractionation of tetra- and
671 trichloroethene during reductive dechlorination by *Sulfurospirillum* ssp. and
672 *Desulfitobacterium* sp. strain PCE-S. *FEMS Microbiol. Ecol.* 62, 98–107.
673 <https://doi.org/10.1111/j.1574-6941.2007.00367.x>

674 Coplen, T.B., 2011. Guidelines and recommended terms for expression of stable-isotope-
675 ratio and gas-ratio measurement results. *Rapid Commun. Mass Spectrom.* 25, 2538–

676 2560. <https://doi.org/10.1002/rcm.5129>

677 Coplen, T.B., 1996. New guidelines for reporting stable hydrogen, carbon, and oxygen
678 isotope-ratio data. *Geochim. Cosmochim. Acta* 60, 3359–3360.
679 [https://doi.org/10.1016/0016-7037\(96\)00263-3](https://doi.org/10.1016/0016-7037(96)00263-3)

680 da Lima, G.P., Sleep, B.E., 2010. The impact of carbon tetrachloride on an anaerobic
681 methanol-degrading microbial community. *Water. Air. Soil Pollut.* 212, 357–368.
682 <https://doi.org/10.1007/s11270-010-0350-z>

683 Ding, C., Zhao, S., He, J., 2014. A *Desulfitobacterium* sp. strain PR reductively
684 dechlorinates both 1,1,1-trichloroethane and chloroform. *Environ. Microbiol.* 16,
685 3387–3397. <https://doi.org/10.1111/1462-2920.12387>

686 Egli, C., Stromeyer, S., Cook, A.M., Leisinger, T., 1990. Transformation of tetra- and
687 trichloromethane to CO₂ by anaerobic bacteria is a non-enzymic process. *FEMS*
688 *Microbiol. Lett.* 68, 207–212. [https://doi.org/10.1016/0378-1097\(90\)90152-G](https://doi.org/10.1016/0378-1097(90)90152-G)

689 Egli, C., Tschan, T., Scholtz, R., Cook, A.M., Leisinger, T., 1988. Transformation of
690 tetrachloromethane to dichloromethane and carbon-dioxide by *Acetobacterium-*
691 *Woodii*. *Appl. Environ. Microbiol.* 54, 2819–2824.

692 Elsner, M., 2010. Stable isotope fractionation to investigate natural transformation
693 mechanisms of organic contaminants: principles, prospects and limitations. *J.*
694 *Environ. Monit.* 12, 2005–2031. <https://doi.org/10.1039/c0em00277a>

695 European Commission, 2012. Priority Substances and Certain Other Pollutants according
696 to Annex II of Directive 2008/105/EC [WWW Document]. URL
697 http://ec.europa.eu/environment/water/water-framework/priority_substances.htm
698 (accessed 10.31.17).

699 Gälli, R., McCarty, P.L., 1989. Biotransformation of 1,1,1-trichloroethane,
700 trichloromethane, and tetrachloromethane by a *Clostridium* sp. *Appl. Environ.*
701 *Microbiol.* 55, 837–844.

702 Gribble, G.W., 2010. Naturally Occurring Organohalogen Compounds - A
703 Comprehensive Update, *Asian Journal of WTO and International Health Law and*
704 *Policy*, *Fortschritte der Chemie organischer Naturstoffe / Progress in the Chemistry*
705 *of Organic Natural Products*. Springer Vienna, Vienna. [https://doi.org/10.1007/978-](https://doi.org/10.1007/978-3-211-99323-1)
706 [3-211-99323-1](https://doi.org/10.1007/978-3-211-99323-1)

707 Grostern, A., Duhamel, M., Dworatzek, S., Edwards, E., 2010. Chloroform respiration to
708 dichloromethane by a *Dehalobacter* population. *Environ. Microbiol.* 12, 1053–1060.
709 <https://doi.org/10.1111/j.1462-2920.2009.02150.x>

710 Heckel, B., Cretnik, S., Kliegman, S., Shouakar-Stash, O., McNeill, K., Elsner, M.,
711 2017a. Reductive outer-sphere single electron transfer is an exception rather than the
712 rule in natural and engineered chlorinated ethene dehalogenation. *Environ. Sci.*
713 *Technol.* 51, 9663–9673. <https://doi.org/10.1021/acs.est.7b01447>

714 Heckel, B., Phillips, E., Edwards, E., Sherwood Lollar, B., Elsner, M., Manefield, M.J.,
715 Lee, M., 2019. Reductive dehalogenation of trichloromethane by two different
716 *Dehalobacter restrictus* strains reveal opposing dual element isotope effects.
717 *Environ. Sci. Technol.* 53, 2332–2343. <https://doi.org/10.1021/acs.est.8b03717>

718 Heckel, B., Rodríguez-Fernández, D., Torrentó, C., Meyer, A.H., Palau, J., Domènech,
719 C., Rosell, M., Soler, A., Hunkeler, D., Elsner, M., 2017b. Compound-specific
720 chlorine isotope analysis of tetrachloromethane and trichloromethane by gas
721 chromatography-isotope ratio mass spectrometry vs gas chromatography-
722 quadrupole mass spectrometry: method development and evaluation of precision and

723 trueuess. Anal. Chem. 89, 3411–3420.
724 <https://doi.org/10.1021/acs.analchem.6b04129>

725 Heraty, L.J., Fuller, M., Huang, L., Abrajano, T., Sturchio, N., 1999. Isotopic
726 fractionation of carbon and chlorine by microbial degradation of dichloromethane.
727 *Org. Geochem.* 30, 793–799. [https://doi.org/10.1016/S0146-6380\(99\)00062-5](https://doi.org/10.1016/S0146-6380(99)00062-5)

728 Hermon, L., Denonfoux, J., Hellal, J., Jouliau, C., Ferreira, S., Vuilleumier, S., Imfeld,
729 G., 2018. Dichloromethane biodegradation in multi-contaminated groundwater:
730 Insights from biomolecular and compound-specific isotope analyses. *Water Res.*
731 142, 217–226. <https://doi.org/10.1016/j.watres.2018.05.057>

732 Holt, B.D., Sturchio, N.C., Abrajano, T., Heraty, L.J., 1997. Conversion of chlorinated
733 volatile organic compounds to carbon dioxide and methyl chloride for isotopic
734 analysis of carbon and chlorine. *Anal. Chem.* 69, 2727–2733.
735 <https://doi.org/10.1021/ac961096b>

736 Hunkeler, D., Meckenstock, R.U., Lollar, B.S., Schmidt, T.C., Wilson, J.T., 2008. A
737 guide for assessing biodegradation and source identification of organic ground water
738 contaminants using compound specific isotope analysis (CSIA), U.S. Environmental
739 Protection Agency. Washington, D.C., EPA/600/R-08/148.

740 Hunkeler, D., Van Breukelen, B.M., Elsner, M., 2009. Modeling chlorine isotope trends
741 during sequential transformation of chlorinated ethenes. *Environ. Sci. Technol.* 43,
742 6750–6756. <https://doi.org/10.1021/es900579z>

743 IARC, 2018. List of classifications, Volumes 1-122 [WWW Document]. IARC Monogr.
744 Eval. Carcinog. Risks to Humans. URL [https://monographs.iarc.fr/list-of-](https://monographs.iarc.fr/list-of-classifications-volumes/)
745 [classifications-volumes/](https://monographs.iarc.fr/list-of-classifications-volumes/) (accessed 10.6.18).

746 IARC, 2016. Some chemicals used as solvents and in polymer manufacture, IARC
747 Monographs on the Evaluation of Carcinogenic Risks to Humans. Lyon.

748 Jeannotat, S., Hunkeler, D., 2012. Chlorine and carbon isotopes fractionation during
749 volatilization and diffusive transport of trichloroethene in the unsaturated zone.
750 Environ. Sci. Technol. 46, 3169–3176. <https://doi.org/10.1021/es203547p>

751 Jendrzewski, N., Eggenkamp, H.G.M., Coleman, M. L., 2001. Characterisation of
752 chlorinated hydrocarbons from chlorine and carbon isotopic compositions: Scope of
753 application to environmental problems. Appl. Geochemistry 16, 1021–1031.
754 [https://doi.org/10.1016/S0883-2927\(00\)00083-4](https://doi.org/10.1016/S0883-2927(00)00083-4)

755 Justicia-Leon, S.D., Higgins, S., Mack, E.E., Griffiths, D.R., Tang, S., Edwards, E.,
756 Löffler, F.E., 2014. Bioaugmentation with distinct Dehalobacter strains achieves
757 chloroform detoxification in microcosms. Environ. Sci. Technol. 48, 1851–1858.
758 <https://doi.org/10.1021/es403582f>

759 Justicia-Leon, S.D., Ritalahti, K.M., Mack, E.E., Löffler, F.E., 2012. Dichloromethane
760 fermentation by a Dehalobacter sp. in an enrichment culture derived from pristine
761 river sediment. Appl. Environ. Microbiol. 78, 1288–1291.
762 <https://doi.org/10.1128/AEM.07325-11>

763 Kampara, M., Thullner, M., Richnow, H.H., Harms, H., Wick, L.Y., 2008. Impact of
764 bioavailability restrictions on microbially induced stable isotope fractionation. 2.
765 Experimental evidence. Environ. Sci. Technol. 42, 6552–6558.
766 <https://doi.org/10.1021/es702781x>

767 Kaufmann, R., Long, A., Bentley, H., Davis, S., 1984. Natural chlorine isotope variations.
768 Nature 309, 338–340. <https://doi.org/10.1038/309338a0>

769 Kleindienst, S., Chourey, K., Chen, G., Murdoch, R.W., Higgins, S.A., Iyer, R.,
770 Campagna, S.R., Mack, E.E., Seger, E.S., Hettich, R.L., Löffler, F.E., 2019.
771 Proteogenomics reveals novel reductive dehalogenases and methyltransferases
772 expressed during anaerobic dichloromethane metabolism. *Appl. Environ. Microbiol.*
773 85. <https://doi.org/10.1128/AEM.02768-18>

774 Kleindienst, S., Higgins, S.A., Tsementzi, D., Chen, G., Konstantinidis, K.T., Mack, E.E.,
775 Löffler, F.E., 2017. ‘*Candidatus Dichloromethanomonas elyunquensis*’ gen. nov.,
776 sp. nov., a dichloromethane-degrading anaerobe of the Peptococcaceae family. *Syst.*
777 *Appl. Microbiol.* 40, 150–159. <https://doi.org/10.1016/j.syapm.2016.12.001>

778 Klindworth, A., Pruesse, E., Schweer, T., Peplies, J., Quast, C., Horn, M., Glöckner, F.O.,
779 2013. Evaluation of general 16S ribosomal RNA gene PCR primers for classical and
780 next-generation sequencing-based diversity studies. *Nucleic Acids Res.* 41, e1–e1.
781 <https://doi.org/10.1093/nar/gks808>

782 Krone, U., Laufer, K., Thauer, R.K., Hogenkamp, H.P.C., 1989a. Coenzyme F430 as a
783 possible catalyst for the reductive dehalogenation of chlorinated C1 hydrocarbons in
784 methanogenic bacteria. *Biochemistry* 28, 10061–10065.
785 <https://doi.org/10.1021/bi00452a027>

786 Krone, U., Thauer, R.K., Hogenkamp, H.P.C., 1989b. Reductive dehalogenation of
787 chlorinated C1-hydrocarbons mediated by corrinoids. *Biochemistry* 28, 4908–4914.
788 <https://doi.org/10.1021/bi00437a057>

789 Lee, M., Low, A., Zemb, O., Koenig, J., Michaelsen, A., Manefield, M.J., 2012. Complete
790 chloroform dechlorination by organochlorine respiration and fermentation. *Environ.*
791 *Microbiol.* 14, 883–894. <https://doi.org/10.1111/j.1462-2920.2011.02656.x>

792 Lee, M., Wells, E., Wong, Y.K., Koenig, J., Adrian, L., Richnow, H.H., Manefield, M.J.,

793 2015. Relative contributions of dehalobacter and zerovalent iron in the degradation
794 of chlorinated methanes. *Environ. Sci. Technol.* 49, 4481–4489.
795 <https://doi.org/10.1021/es5052364>

796 Liang, X., Howlett, M.R., Nelson, J.L., Grant, G., Dworatzek, S., Lacrampe-Couloume,
797 G., Zinder, S.H., Edwards, E., Sherwood Lollar, B., 2011. Pathway-dependent
798 isotope fractionation during aerobic and anaerobic degradation of
799 monochlorobenzene and 1,2,4-trichlorobenzene. *Environ. Sci. Technol.* 45, 8321–
800 8327. <https://doi.org/10.1021/es201224x>

801 Löffler, F.E., Sanford, R.A., Ritalahti, K.M., 2005. Enrichment, cultivation, and detection
802 of reductively dechlorinating bacteria. *Methods Enzymol.* 397, 77–111.
803 [https://doi.org/10.1016/S0076-6879\(05\)97005-5](https://doi.org/10.1016/S0076-6879(05)97005-5)

804 Mägli, A., Messmer, M., Leisinger, T., 1998. Metabolism of dichloromethane by the strict
805 anaerobe *Dehalobacterium formicoaceticum*. *Appl. Environ. Microbiol.* 64, 646–
806 650.

807 Marshall, K.A., Pottenger, L.H., 2016. Chlorocarbons and Chlorohydrocarbons, in: Ley,
808 C. (Ed) *Kirk-Othmer Encyclopedia of Chemical Technology*. John Wiley & Sons,
809 Inc., Hoboken, NJ, USA, pp. 1–29.
810 <https://doi.org/10.1002/0471238961.1921182218050504.a01.pub3>

811 Martín-González, L., Mortan, S.H., Rosell, M., Parladé, E., Martínez-Alonso, M., Gaju,
812 N., Caminal, G., Adrian, L., Marco-Urrea, E., 2015. Stable carbon isotope
813 fractionation during 1,2-dichloropropane-to-propene transformation by an
814 enrichment culture containing *Dehalogenimonas* strains and a *dcpA* gene. *Environ.*
815 *Sci. Technol.* 49, 8666–74. <https://doi.org/10.1021/acs.est.5b00929>

816 Mikesell, M.D., Boyd, S.A., 1990. Dechlorination of chloroform by *Methanosarcina*

817 strains. *Appl. Environ. Microbiol.* 56, 1198–1201.

818 Mortan, S.H., Martín-González, L., Vicent, T., Caminal, G., Nijenhuis, I., Adrian, L.,
819 Marco-Urrea, E., 2017. Detoxification of 1,1,2-trichloroethane to ethene in a
820 bioreactor co-culture of *Dehalogenimonas* and *Dehalococcoides mccartyi* strains. *J.*
821 *Hazard. Mater.* 331, 218–225. <https://doi.org/10.1016/j.jhazmat.2017.02.043>

822 Muller, E.E.L., Bringel, F., Vuilleumier, S., 2011. Dichloromethane-degrading bacteria
823 in the genomic age. *Res. Microbiol.* 162, 869–876.
824 <https://doi.org/10.1016/j.resmic.2011.01.008>

825 Mundle, S.O.C., Vandersteen, A.A., Lacrampe-Couloume, G., Kluger, R., Sherwood
826 Lollar, B., 2013. Pressure-monitored headspace analysis combined with compound-
827 specific isotope analysis to measure isotope fractionation in gas-producing reactions.
828 *Rapid Commun. Mass Spectrom.* 27, 1778–1784. <https://doi.org/10.1002/rcm.6625>

829 Nikolausz, M., Nijenhuis, I., Ziller, K., Richnow, H.H., Kastner, M., 2006. Stable carbon
830 isotope fractionation during degradation of dichloromethane by methylotrophic
831 bacteria. *Environ. Microbiol.* 8, 156–164. <https://doi.org/10.1111/j.1462-2920.2005.00878.x>

833 Palau, J., Jamin, P., Badin, A., Vanhecke, N., Haerens, B., Brouyère, S., Hunkeler, D.,
834 2016. Use of dual carbon–chlorine isotope analysis to assess the degradation
835 pathways of 1,1,1-trichloroethane in groundwater. *Water Res.* 92, 235–243.
836 <https://doi.org/10.1016/j.watres.2016.01.057>

837 Palau, J., Yu, R., Mortan, S.H., Shouakar-Stash, O., Rosell, M., Freedman, D.L., Sbarbati,
838 C., Fiorenza, S., Aravena, R., Marco-Urrea, E., Elsner, M., Soler, A., Hunkeler, D.,
839 2017. Distinct dual C–Cl isotope fractionation patterns during anaerobic
840 biodegradation of 1,2-dichloroethane: potential to characterize microbial

841 degradation in the field. *Environ. Sci. Technol.* 51, 2685–2694.
842 <https://doi.org/10.1021/acs.est.6b04998>

843 Renpenning, J., Rapp, I., Nijenhuis, I., 2015. Substrate hydrophobicity and cell
844 composition influence the extent of rate limitation and masking of isotope
845 fractionation during microbial reductive dehalogenation of chlorinated ethenes.
846 *Environ. Sci. Technol.* 49, 4293–4301. <https://doi.org/10.1021/es506108j>

847 Rodríguez-Fernández, D., Torrentó, C., Guivernau, M., Viñas, M., Hunkeler, D., Soler,
848 A., Domènech, C., Rosell, M., 2018a. Vitamin B 12 effects on chlorinated methanes-
849 degrading microcosms: Dual isotope and metabolically active microbial populations
850 assessment. *Sci. Total Environ.* 621, 1615–1625.
851 <https://doi.org/10.1016/j.scitotenv.2017.10.067>

852 Rodríguez-Fernández, D., Torrentó, C., Palau, J., Marchesi, M., Soler, A., Hunkeler, D.,
853 Domènech, C., Rosell, M., 2018b. Unravelling long-term source removal effects and
854 chlorinated methanes natural attenuation processes by C and Cl stable isotopic
855 patterns at a complex field site. *Sci. Total Environ.* 645, 286–296.
856 <https://doi.org/10.1016/j.scitotenv.2018.07.130>

857 Sherwood Lollar, Barbara, Hirschorn, S., Mundle, S.O.C., Grostern, A., Edwards, E.,
858 Lacrampe-Couloume, G., Sherwood Lollar, B., 2010. Insights into enzyme kinetics
859 of chloroethane biodegradation using compound specific stable isotopes. *Environ.*
860 *Sci. Technol.* 44, 7498–7503. <https://doi.org/10.1021/es101330r>

861 Shouakar-Stash, O., Drimmie, R.J., Zhang, M., Frappe, S.K., 2006. Compound-specific
862 chlorine isotope ratios of TCE, PCE and DCE isomers by direct injection using CF-
863 IRMS. *Appl. Geochemistry* 21, 766–781.
864 <https://doi.org/10.1016/j.apgeochem.2006.02.006>

865 Shouakar-Stash, O., Frappe, S.K., Drimmie, R.J., 2003. Stable hydrogen, carbon and
866 chlorine isotope measurements of selected chlorinated organic solvents. *J. Contam.*
867 *Hydrol.* 60, 211–228. [https://doi.org/10.1016/S0169-7722\(02\)00085-2](https://doi.org/10.1016/S0169-7722(02)00085-2)

868 Tang, S., Edwards, E., 2013. Identification of Dehalobacter reductive dehalogenases that
869 catalyse dechlorination of chloroform, 1,1,1-trichloroethane and 1,1-
870 dichloroethane. *Philos. Trans. R. Soc. B Biol. Sci.* 368.
871 <https://doi.org/10.1098/rstb.2012.0318>

872 Thullner, M., Kampara, M., Richnow, H.H., Harms, H., Wick, L.Y., 2008. Impact of
873 bioavailability restrictions on microbially induced stable isotope fractionation. 1.
874 Theoretical calculation. *Environ. Sci. Technol.* 42, 6544–6551.
875 <https://doi.org/10.1021/es702782c>

876 Torgonskaya, M.L., Zyakun, A.M., Trotsenko, Y.A., Laurinavichius, K.S., Kümmel, S.,
877 Vuilleumier, S., Richnow, H.H., 2019. Individual stages of bacterial
878 dichloromethane degradation mapped by carbon and chlorine stable isotope analysis.
879 *J. Environ. Sci.* 78, 147–160. <https://doi.org/10.1016/j.jes.2018.09.008>

880 Torrentó, C., Palau, J., Rodríguez-Fernández, D., Heckel, B., Meyer, A., Domènech, C.,
881 Rosell, M., Soler, A., Elsner, M., Hunkeler, D., 2017. Carbon and chlorine isotope
882 fractionation patterns associated with different engineered chloroform
883 transformation reactions. *Environ. Sci. Technol.* 51, 6174–6184.
884 <https://doi.org/10.1021/acs.est.7b00679>

885 Trueba-Santiso, A., Parladé, E., Rosell, M., Lliros, M., Mortan, S.H., Martínez-Alonso,
886 M., Gaju, N., Martín-González, L., Vicent, T., Marco-Urrea, E., 2017. Molecular
887 and carbon isotopic characterization of an anaerobic stable enrichment culture
888 containing Dehalobacterium sp. during dichloromethane fermentation. *Sci. Total*

889 Environ. 581–582, 640–648. <https://doi.org/10.1016/j.scitotenv.2016.12.174>

890 van Warmerdam, E.M.M., Frappe, S.K.K., Aravena, R., Drimmie, R.J., Flatt, H., Cherry,
891 J.A. a, 1995. Stable chlorine and carbon isotope measurement of selected chlorinated
892 organic solvents. *Appl. Geochem.* 10, 547–552. [https://doi.org/10.1016/0883-](https://doi.org/10.1016/0883-2927(95)00025-9)
893 [2927\(95\)00025-9](https://doi.org/10.1016/0883-2927(95)00025-9)

894 Wanner, P., Parker, B.L., Chapman, S.W., Lima, G., Gilmore, A., Mack, E.E., Aravena,
895 R., 2018. Identification of degradation pathways of chlorohydrocarbons in saturated
896 low-permeability sediments using compound-specific isotope analysis. *Environ. Sci.*
897 *Technol.* 52, 7296–7306. <https://doi.org/10.1021/acs.est.8b01173>

898 Weathers, L.J., Parkin, G.F., 2000. Toxicity of chloroform biotransformation to
899 methanogenic bacteria. *Environ. Sci. Technol.* 34, 2764–2767.
900 <https://doi.org/10.1021/es990948x>

901 Wei, K., Grostern, A., Chan, W.W.M., Richardson, R.E., Edwards, E.A., 2016. Electron
902 acceptor interactions between organohalide-respiring bacteria: cross-feeding,
903 competition, and inhibition, in: L. Adrian and F.E. Löffler (Ed) *Organohalide-*
904 *Respiring Bacteria*. Springer Berlin Heidelberg, Berlin, Heidelberg, pp. 283–308.
905 https://doi.org/10.1007/978-3-662-49875-0_13

906 Wong, Y.K., Holland, S.I., Ertan, H., Manefield, M.J., Lee, M., 2016. Isolation and
907 characterization of *Dehalobacter* sp. strain UNSWDHB capable of chloroform and
908 chlorinated ethane respiration. *Environ. Microbiol.* 18, 3092–3105.
909 <https://doi.org/10.1111/1462-2920.13287>

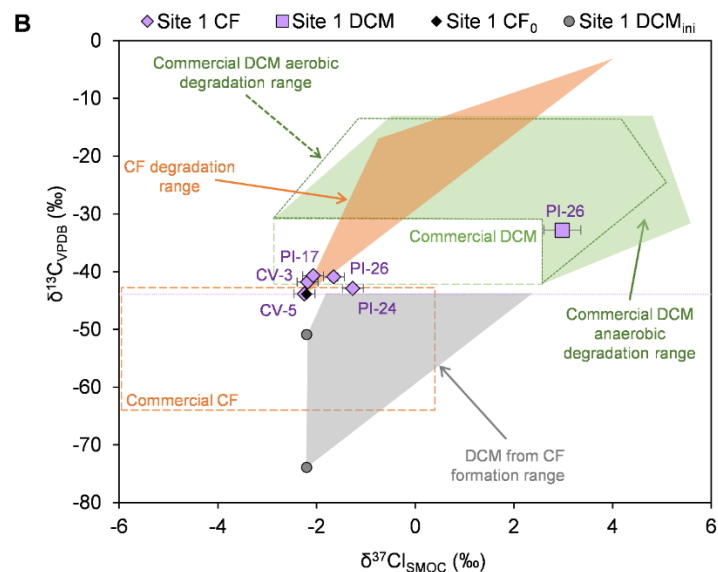
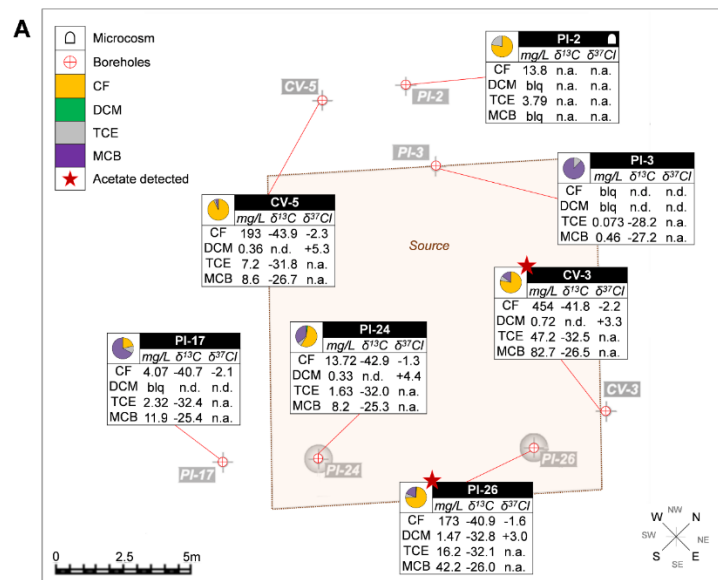
910

911

912 **FIGURE AND CAPTIONS**

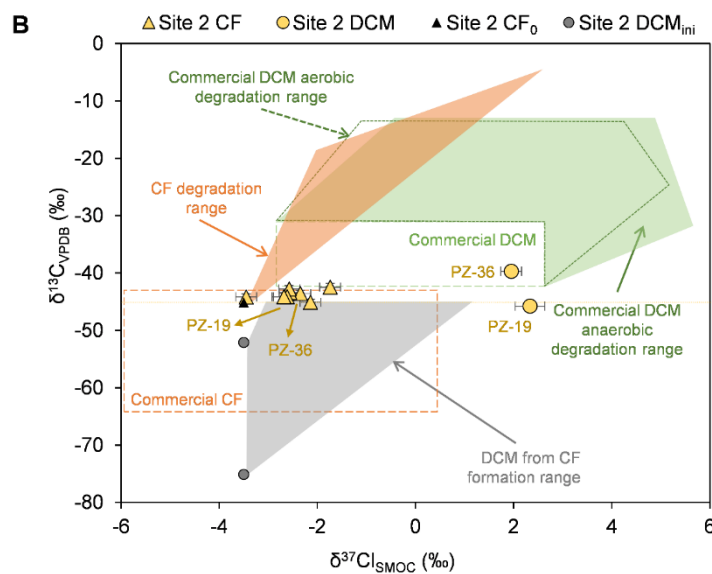
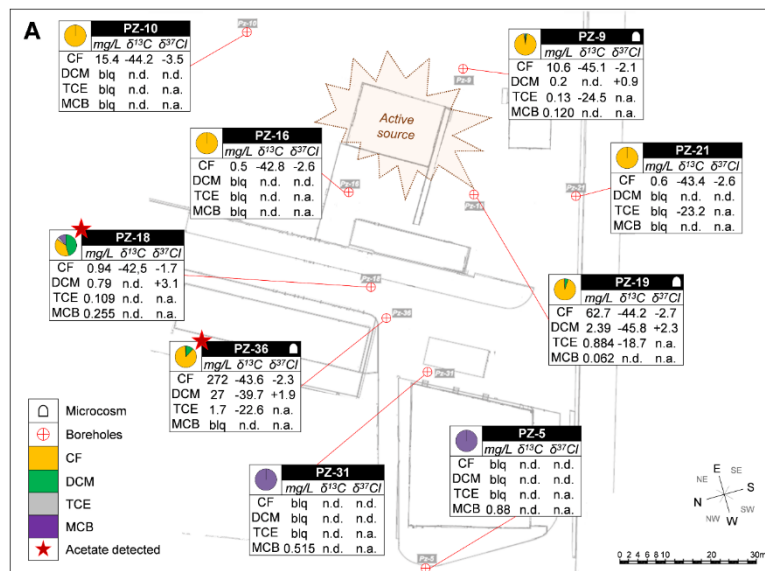
913

914 **Figure 1.** (A) Concentrations (in mg/L) and $\delta^{13}\text{C}$ and $\delta^{37}\text{Cl}$ compositions (in ‰) of CF,
 915 DCM, TCE and MCB from Site 1. Pie charts show the molar distribution of contaminants
 916 at each well. Detailed concentrations (in μM) and isotopic compositions are available in
 917 SI sections G and H, respectively. “n.d.” means “could not be determined based on their
 918 low concentration”; “n.a.” means “not analysed”. (B) Dual C–Cl isotopic assessment for
 919 DCM and CF field data from Site 1. Both CF_0 and the range for DCM_{ini} are represented.
 920 Green and orange dashed rectangles depict the $\delta^{13}\text{C}$ and $\delta^{37}\text{Cl}$ ranges of commercial DCM
 921 and CF solvents, respectively (see Table 2 for details).



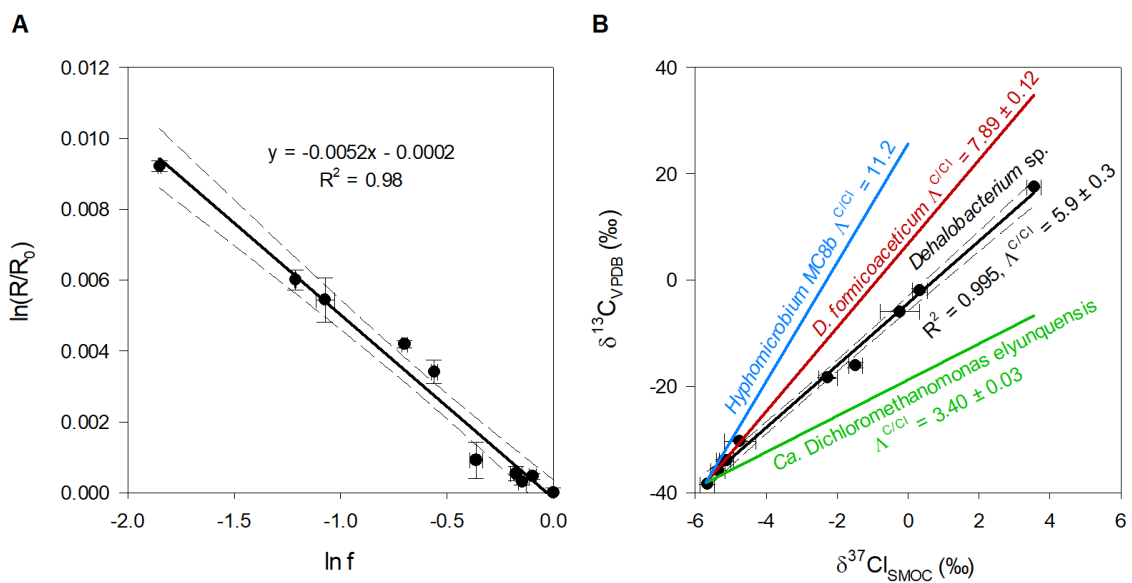
922

923 **Figure 2.** (A) Concentrations (in mg/L) and $\delta^{13}\text{C}$ and $\delta^{37}\text{Cl}$ compositions (in ‰) of CF,
 924 DCM, TCE and MCB from Site 2. Pie charts show the molar distribution of contaminants
 925 at each well. Detailed concentrations (in μM) and isotopic compositions are available in
 926 SI sections G and H, respectively. “n.d.” means “could not be determined based on their
 927 low concentration”; “n.a.” means “not analysed”. (B) Dual C–Cl isotopic assessment for
 928 DCM and CF field data from Site 2. Both CF_0 and the range for DCM_{ini} are represented.
 929 Green and orange dashed rectangles depict the $\delta^{13}\text{C}$ and $\delta^{37}\text{Cl}$ ranges of commercial DCM
 930 and CF solvents, respectively (see Table 2 for details).



931

932 **Figure 3.** Double logarithmic Rayleigh plot for chlorine isotope data (A) and dual C–Cl
 933 isotope plot (B) for the anaerobic degradation of DCM by the *Dhb* containing culture
 934 investigated in this study. Solid black lines for the *Dhb* culture in each panel depict the
 935 corresponding linear regression and dashed lines represent the associated 95% CI. In
 936 panel B, the trend lines reported for DCM degradation by *Hyphomicrobium* strain MC8b
 937 (Heraty et al., 1999), *Dhb f.* and *D. elyunquensis* (Chen et al., 2018) are shown for
 938 comparison. Data points show the error bars from duplicate measurements.



939

940

941 TABLES

942 Table 1. ϵ_C , ϵ_{Cl} and $\Lambda^{C/Cl}$ of DCM and CF degradation by several mechanisms^a.

DCM	ϵ_C (‰)	ϵ_{Cl} (‰)	$\Lambda^{C/Cl}$	Reference
Mixed culture containing <i>Dehalobacterium</i> sp. (<i>Dhb</i>)	-31 ± 3*	-5.2 ± 0.6	+5.9 ± 0.3	This study and re-calculated from Trueba-Santiso et al. (2017)*
<i>Dehalobacterium formicoaceticum</i> (<i>Dhb</i> f.)	-42.4 ± 0.7	-5.3 ± 0.1	+7.89 ± 0.12	Chen et al. (2018)
Consortium RM harboring <i>Ca. Dichloromethanomonas elyunquensis</i>	-18.3 ± 0.2	-5.2 ± 0.1	+3.40 ± 0.03	Chen et al. (2018)
Mixed culture containing <i>Dehalobacter</i> sp. (DCMD)	-16 ± 2	n.a. ^b	n.a.	Lee et al. (2015)
<i>Hyphomicrobium</i> sp. strain MC8b	-42.4 ^{c,d}	-3.8 ^{c,d}	+11.2 ^{c,d}	Heraty et al. (1999)
<i>Hyphomicrobium</i> strains, <i>Methylobacterium</i> , <i>Methylopila</i> , <i>Methylophilus</i> , and <i>Methylorhabdus</i> strains	-41.2 to -66.3 ^d	n.a.	n.a.	Nikolausz et al. (2006)
<i>Hyphomicrobium</i> strains	-45.8 to -61.0 ^e	n.a.	n.a.	Nikolausz et al. (2006)
	-22 to -46 ^d	n.a.	n.a.	Hermon et al. (2018)
	-26 ± 5 ^e			Hermon et al. (2018)
<i>Methylobacterium extorquens</i> DM4 (average between high and low density cell suspensions)	-66.6 ^{d,f}	-7.0 ^{d,f}	+9.5 ^{d,f}	Torgonskaya et al. (2019)
DM4 DCM dehalogenase (average between high and low activity)	-48.4 ^{d,f}	-5.7 ^{d,f}	+8.5 ^{d,f}	Torgonskaya et al. (2019)
DM11 DCM dehalogenase (average between high and low activity)	-45.4 ^{d,f}	-5.6 ^{d,f}	+8.1 ^{d,f}	Torgonskaya et al. (2019)
CF	ϵ_C (‰)	ϵ_{Cl} (‰)	$\Lambda^{C/Cl}$	Reference
Oxidation	-8 ± 1	-0.44 ± 0.06	+17 ± 2	Torrentó et al. (2017)
Alkaline hydrolysis	-57 ± 5	-4.4 ± 0.4	+13.0 ± 0.8	Torrentó et al. (2017)
Hydrogenolysis plus reductive elimination with Fe (0)	-33 ± 11	-3 ± 1	+8 ± 2	Torrentó et al. (2017)
Biodegradation with vitamin B ₁₂	-14 ± 4	-2.4 ± 0.4	+7 ± 1	Rodríguez-Fernández et al. (2018a)
Outer-sphere single electron transfer (OS-SET)	-17.7 ± 0.8	-2.6 ± 0.2	+6.7 ± 0.4	Heckel et al. (2017a)
<i>Dehalobacter</i> strain CF	-28 ± 2	-4.2 ± 0.2	+6.6 ± 0.1	Heckel et al. (2019)
<i>Dehalobacter</i> strain UNSWDHB	-3.1 ± 0.5	+2.5 ± 0.3	-1.2 ± 0.2	Heckel et al. (2019)
Mixed culture containing <i>Dehalobacter</i> strain UNSWDHB	-4.3 ± 0.5	n.a.	n.a.	Lee et al. (2015)

^aUncertainties of ϵ and Λ values correspond to the 95% confidence interval (CI). ^bn.a., values were not analysed. ^c $\Lambda^{C/Cl}$ values were calculated based on reported ϵ_C and ϵ_{Cl} data by the referenced authors. ^dValues were measured under oxidic conditions. ^eValues were measured under nitrate-reducing conditions. ^f ϵ_C and ϵ_{Cl} values were calculated here based on reported α_C and α_{Cl} data ($\epsilon_{C,Cl} = 1/\alpha_{C,Cl} - 1 \cdot 1000$), and the $\Lambda^{C/Cl}$ values from the here estimated ϵ_C and ϵ_{Cl} values ($\Lambda^{C/Cl} \sim \epsilon_C/\epsilon_{Cl}$).

943

944 **Table 2.** $\delta^{13}\text{C}$ and $\delta^{37}\text{Cl}$ (in ‰) of commercial pure-phase CF, DCM, TCE and MCB.

DCM	$\delta^{13}\text{C}$ (‰/VPDB)	$\delta^{37}\text{Cl}$ (‰/SMOC)	Reference
Fisher	-41.71 ± 0.08	-2.7 ± 0.1	This study
Sigma Aldrich	-	$+0.75 \pm 0.05$	This study
SDS	-35.4 ± 0.2	$+1.27 \pm 0.01$	This study
Merck	-39.0 ± 0.1	-	This study
unknown	-39.78 ± 0.08	-	This study
unknown	-	$+1.3 \pm 0.2$	This study
unknown	-	$+2.1 \pm 0.3$	This study
unknown	-31.5 ± 0.3	$+2.13 \pm 0.03$	Jendrzejewski et al. (2001)
unknown	-31.8 ± 0.5	$+2.3 \pm 0.2$	Jendrzejewski et al. (2001)
unknown	-34.19 ± 0.02	$+1.555 \pm 0.005$	Holt et al. (1997)
unknown	-40.4 ± 0.5	-	Holt et al. (1997)
CF	$\delta^{13}\text{C}$ (‰/VPDB)	$\delta^{37}\text{Cl}$ (‰/SMOC)	Reference
Merck ^a	-48.93 ± 0.08	-	This study
Merck ^a	-52.7 ± 0.1	-	This study
Sigma Aldrich	-	-2.6 ± 0.1	This study
Alfa	-47.96 ± 0.06	-5.9 ± 0.2	This study
Alfa	-47.88 ± 0.08	-5.4 ± 0.3	Breider (2013)
unknown	-43.21 ± 0.04	-1.52 ± 0.01	Holt et al. (1997)
Fluka	-48.7 ± 0.1	-3.0 ± 0.2	Rodríguez-Fernández et al. (2018b), Heckel et al. (2017b)
Acros	-49.76 ± 0.08	-	Rodríguez-Fernández et al. (2018b)
unknown	-51.7 ± 0.4	$+0.32 \pm 0.08$	Jendrzejewski et al. (2001)
Fisher	-53.23 ± 0.09	-	Rodríguez-Fernández et al. (2018b)
Sigma Aldrich	-63.6 ± 0.1	-	Breider (2013)
TCE	$\delta^{13}\text{C}$ (‰/VPDB)	$\delta^{37}\text{Cl}$ (‰/SMOC)	Reference
unknown	-25.40 ± 0.03	-	This study
unknown	-27.18 ± 0.01	-1.42 ± 0.10	Holt et al. (1997)
PPG	-27.37 ± 0.09	-2.8 ± 0.1	Shouakar-Stash et al. (2003)
unknown	-27.90 ± 0.08	$+2.0 \pm 0.1$	Jendrzejewski et al. (2001)
StanChem	-29.1 ± 0.1	-3.19 ± 0.07	Shouakar-Stash et al. (2003)
ICI	-31.01 ± 0.09	$+2.71 \pm 0.08$	Shouakar-Stash et al. (2003)
Dow	-31.57 ± 0.01	$+3.55 \pm 0.05$	Shouakar-Stash et al. (2003)
Dow	-31.90 ± 0.05	$+4.1 \pm 0.3$	van Warmerdam et al. (1995)
Sigma Aldrich	-33.49 ± 0.08	$+3.8 \pm 0.1$	Jendrzejewski et al. (2001)
MCB	$\delta^{13}\text{C}$ (‰/VPDB)	$\delta^{37}\text{Cl}$ (‰/SMOC)	Reference
Sigma Aldrich	-27.09 ± 0.07	-	This study
Sigma Aldrich	-25.6^b	-	Liang et al. (2011)

^aSolvent with the same reference number but from different batches. ^b $\delta^{13}\text{C}$ (‰) value for MCB was obtained from a microcosm experiment where changes in $\delta^{13}\text{C}$ by biodegradation of MCB were measured. The initial $\delta^{13}\text{C}$ is not considered to be affected by degradation and, therefore, can be assumed as representative of the commercial MCB. VPDB: Vienna Pee Dee Belemnite, SMOC: Standard Mean Ocean Chloride.